Article

Discovery Medicine 2023; 35(176): 221–232
https://doi.org/10.24976/Discov.Med.202335176.23

Predictive Model for the Diagnosis of Benign/Malignant Complex Cystic and Solid Breast Nodules

Han Liu[1,†], Chun-Jie Hou[1,†], Jing-Lan Tang[1,*], An-Ning Liu[2], Ke-Feng Lu[1], Ying Liu[1], Pei Du[1]

[1]Cancer Center, Department of Ultrasound Medicine, Key Laboratory for Diagnosis and Treatment of Upper Limb Edema and Stasis of Breast Cancer, Zhejiang Provincial People's Hospital, Affiliated People's Hospital, Hangzhou Medical College, 310011 Hangzhou, Zhejiang, China
[2]Department of Ultrasound, Women's Hospital School of Medicine Zhejiang University, 310002 Hangzhou, Zhejiang, China
*Correspondence: tangjinglan_85@163.com (Jing-Lan Tang)
[†]These authors contributed equally.
Published: 2 June 2023

Purpose: To develop an ultrasound predictive model to differentiate between benign and malignant complex cystic and solid nodules (C-SNs).

Methods: A total of 211 patients with complex C-SNs rated as American College of Radiology Breast Imaging Reporting and Data System (ACR BI-RADS) category 4 or 5 on the ultrasound reports were included in the study, from June 2018–2021. Multivariate stepwise logistic regression analysis was used to establish a predictive model, based on clinical and ultrasound features. The diagnostic performance of the model was evaluated by the area under the curve (AUC) of the receiver operating characteristic curve.

Results: A total of 109 breast nodules, including 74 benign nodules (67.89%) and 35 malignant nodules (32.11%), were detected by surgical pathology or puncture biopsy. Multivariate analysis showed that the blood flow (BF) of complex C-SNs ($p = 0.03$), cystic fluid transmission ($p = 0.02$), longitudinal diameter ($p < 0.001$), and age ($p = 0.03$) were independent risk factors for malignant complex cystic and solid breast nodules. The ultrasound model equation was $Z = -12.14 + 2.24 \times X_{12} + 1.97 \times X_{20} + 0.40 \times X_7 + 0.11 \times X_0$; $M = \frac{e^z}{1} + e^z$ (*M* is the malignancy score, $e = 2.72$). The area under the curve (AUC) was 0.89, which indicated good predictive utility for the model.

Conclusions: A prediction model incorporating major risk factors can predict the malignant C-SNs with accuracy.

Keywords: ultrasonography; predictive models; breast cancer; malignant; cystic; solid nodules

Introduction

Breast cancer is one of the most common malignant tumors that affects women [1]. Ultrasound (US) is a sensitive, fast, easy, and non-invasive method for screening for breast cancer [2,3]. The Breast Imaging Reporting and Data system (BI-RADS) applies broadly to the semi-quantitative analysis and prediction of malignant nodules [4]. According to the BI-RADS lexicon, the sonographic features of complex cystic-solid nodules (C-SNs) were defined in the BI-RADS dictionary as a combination of cystic and solid components/cystic lesions with thick walls and thick separations [5,6]. Complex cystic and solid breast lesions are suspected of malignancy and classified as BI-RADS class $\geq$4 [4]. These lesions are diagnosed by biopsy and/or surgical resection [4–7]. However, there is a risk of spread, due to leakage of cystic fluid during percutaneous core needle biopsy, leading to positive margins and/or incomplete surgical excision. Therefore, a non-invasive and accurate diagnosis of C-SNs would decrease the rate of positive margins and re-excision [4,7–9].

The evaluation metrics, including shape, mode of growth, nodule margins, and blood flow (BF) distribution, are standardized features in the BI-RADS classification to predict malignant breast nodules [10]. However, the BI-RADS classification might lead to the underestimation of such nodules [9]. Therefore, when faced with some complex C-SNs, the BI-RADS classification could be insufficient for accurately assessing the malignant nature of nodules. This makes it difficult for surgeons to take further measures (surgery or biopsy) [11]. Hitherto, only a few studies assessed the diagnosis of malignant complex C-SNs of the breast, and different diagnostic results were mentioned in different studies. Kulali *et al.* [11] suggested that the percentage of solid fraction and the morphological and internal echogenic changes of the nodule are likely to be among the predictors of malignant C-SNs. Although there are some studies about the ultrasound features of C-SNs, a relevant predictive model is yet to be established [10].

The present study aimed to develop predictive models, termed the distinguishing risk of malignant C-SNs models, for predicting benign or malignant complex C-SNs.

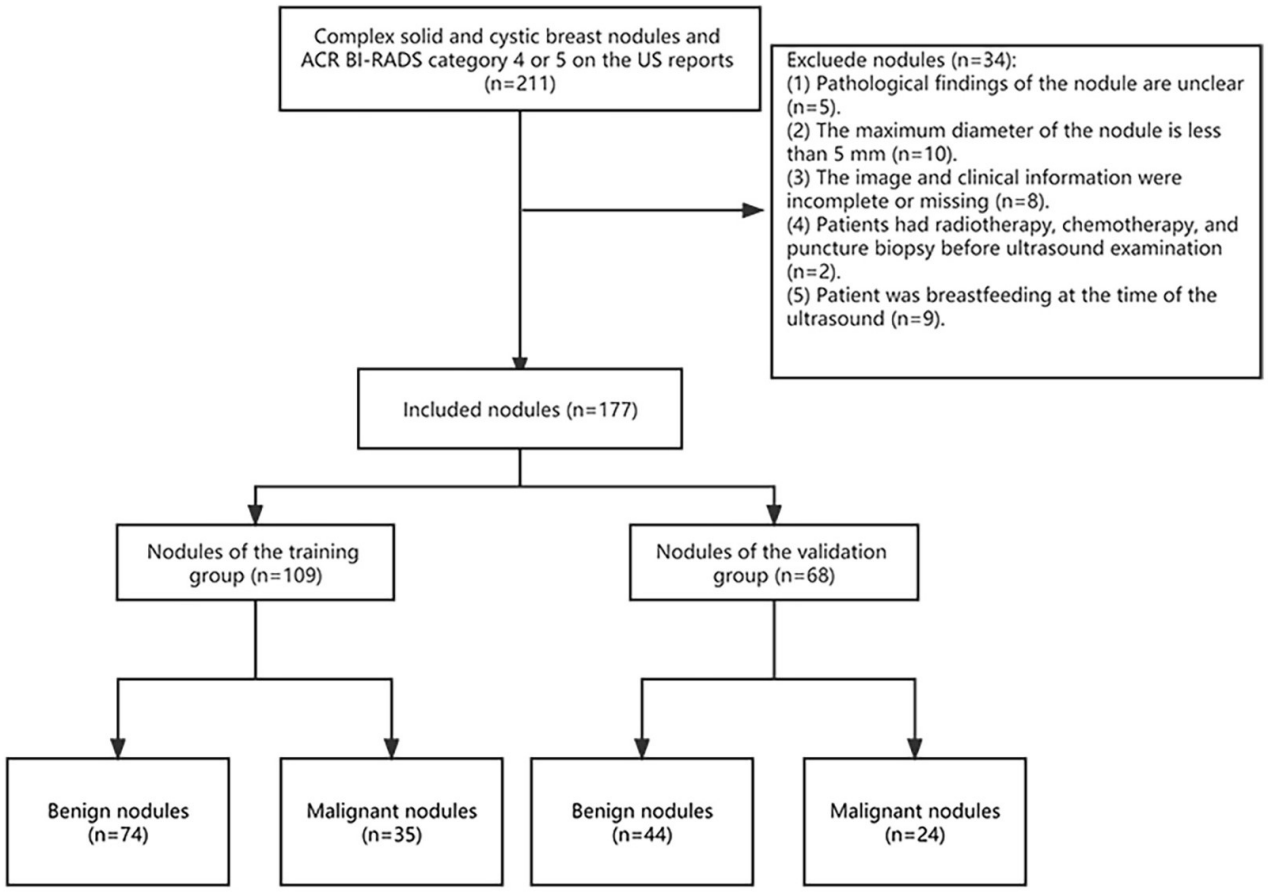

Fig. 1. Flowchart.

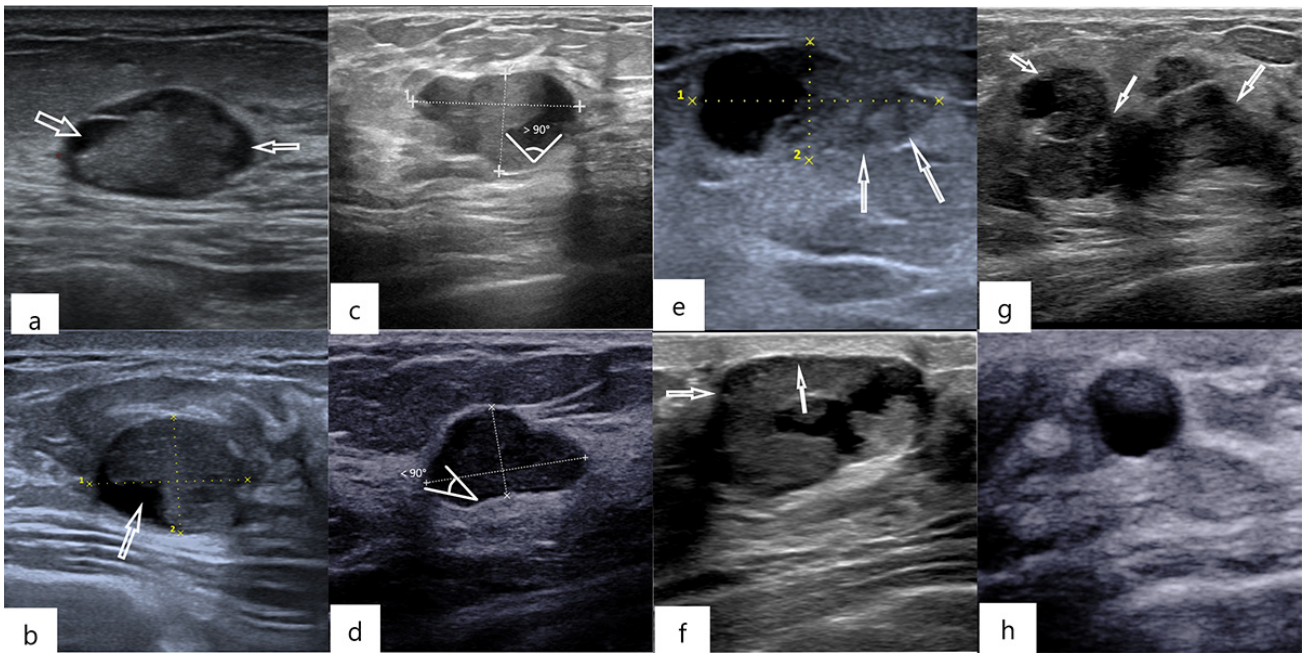

Fig. 2. Images present general US characteristics of nodules. (1) The distribution of cyst-solid components is regular in the surrounding (a) or eccentric (b), and the arrow marks the cystic part. (2) The angle between the solid part and capsule wall is acute (c) or obtuse (d). (3) Demarcation of the solid portion of the attached cystic wall from the peripheral glands is clear (e) or unclear (f), and the arrow marks the demarcation. (4) The lesion shape is irregular (g) or regular (h), and the arrow marks irregular borders.

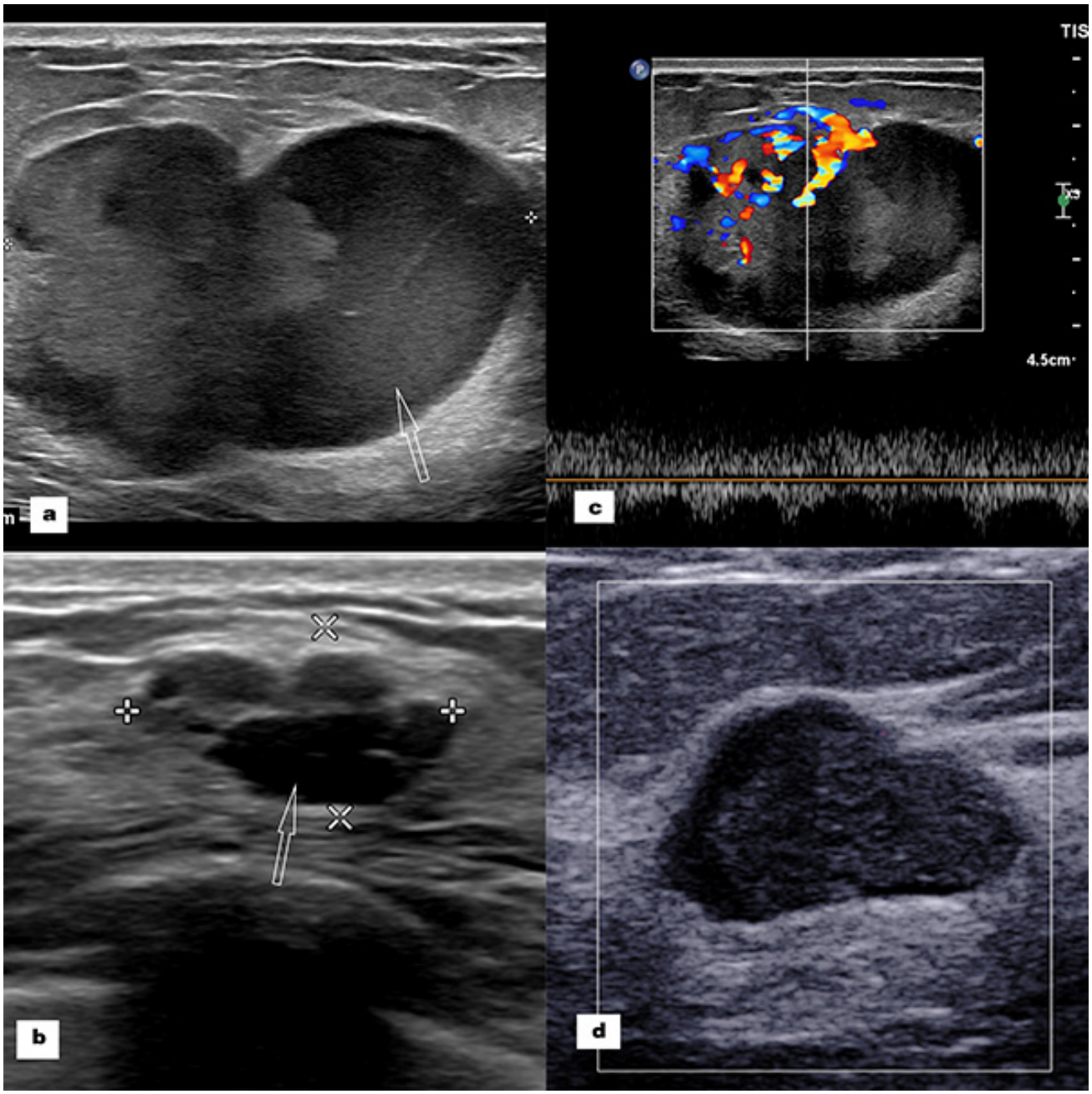

Fig. 3. Images present significant US characteristics of the nodules. (1) Cystic fluid transmission is bad (a) and clarity (b), and the arrow marks the cystic part. (2) Internal vascularity is abundant (c) or absent (d).

Materials and Methods

Patients

A total of 211 nodules in 205 patients from June 2018–2021 were included in this study and the data collection was consistent with relevant ethical requirements [12].

The inclusion criteria were as follows:

(a) Ultrasound (US) was performed and complete ultrasound images were obtained before procedure or biopsy;

(b) The nodules were described as complex C-SNs and BI-RADS category 4 or 5 on the US reports;

(c) All nodules were received surgery or biopsied with complete pathological findings.

The exclusion criteria were as follows:

(a) Pathological findings of the nodule were unclear (n = 5 (15%));

(b) The minimal diameter of the nodule was <5 mm (n = 10 (29%)) (Unclear structure within small nodules);

(c) The imaging and clinical information were incomplete or missing (n = 8 (24%));

(d) Patients received radiotherapy, chemotherapy, and puncture biopsy before US examination (n = 2 (6%));

(e) Patient was breastfeeding at the time of US (n = 9 (26%)).

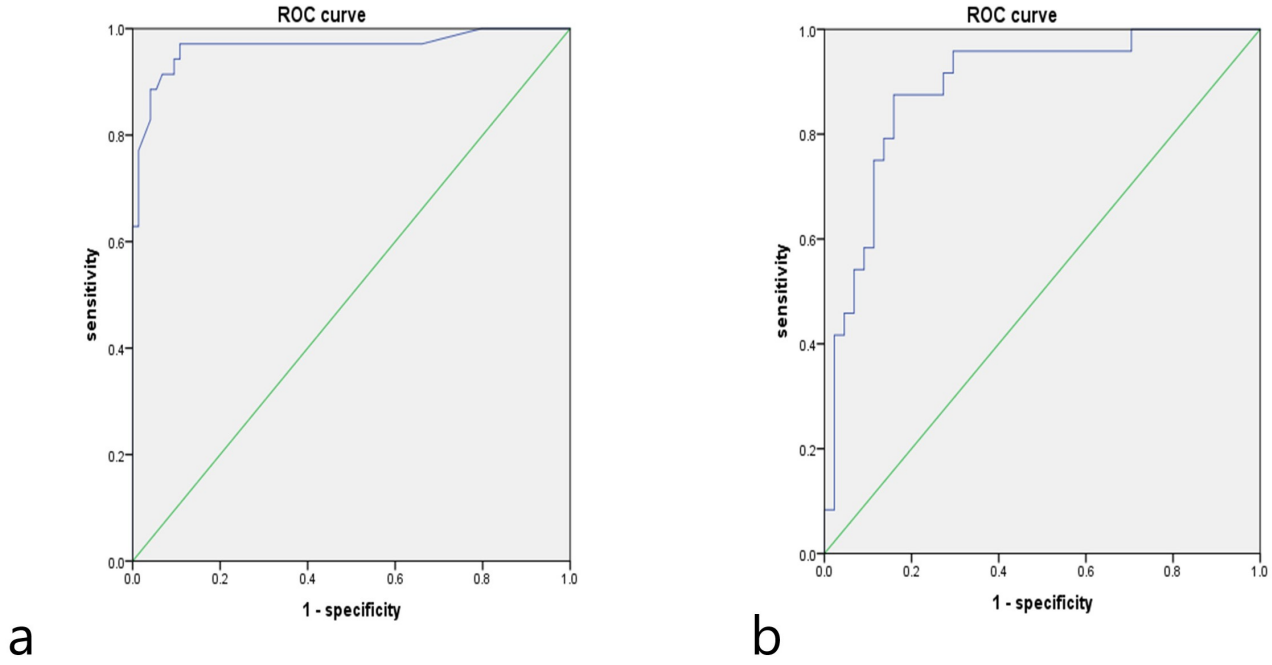

Fig. 4. Receiver operator curve (ROC) for predictive equations for the benign and malignant cystic-solid nodules of the breast. (a) Receiver operator curve (ROC) of training group, the AUC is 0.92 (95% CI, 0.88, 0.99). (b) Receiver operator curve (ROC) curve of the validation group, the AUC is 0.89 (95% CI, 0.81, 0.97).

After screening, 177 nodules from 170 patients were eligible for this study. A total of 109 nodules collected in 2018–2020 were selected for the model training group, and 68 nodules collected in 2021 comprised the validation group. According to the BI-RADS US lexicon, a total of 177 nodules were classified as follows: 144 (81.4%) nodules were category 4a, 15 (8.4%) nodules were category 4b, 10 (5.6%) nodules were category 4c, and 8 (4.5%) nodules were category 5. The flowchart is shown in Fig. 1. Pathology results were given by a pathologist and reviewed by another senior pathologist.

Data Collection

The relevant clinical data were collected and defined as the independent variable X, including age (X_0), height (X_1), weight (X_2), history of lactation (X_3), history of menopause (X_4), and family history of breast cancer (X_5). The above variables are defined in Table 1.

Ultrasonographic Image Features

(a) Instrument selection: The images of patients and cases in this study were acquired using multiple ultrasonic diagnostic apparatus from the US Department of Ultrasound Medicine, Zhejiang Provincial People's Hospital, including Philips Epic 5 ultrasound system (USD18C1531, Philips Medical Systems, Bothell, WA, USA), Supersonic Aixplorer ultrasound system (CE14PS76, Supersonic Imagine, Aix-en-Provence, France), Mindray Resona 7S (7Y-71000028, Mindray, Shenzhen, China), and Mindray DC-8 (QE-5C003984, Mindray, Shenzhen, China). Images were acquired using high-frequency linear array transducer with a central frequency of $\geq$12 MHz, and the machine settings were optimized to obtain high-quality grayscale and color Doppler images of the target lesions. The maximum diameter of the lesion was measured on the largest cross-section.

(b) Ultrasonic feature selection and definition: According to BI-RADS, the morphology, growth orientation, margins (X_8), echogenic pattern, posterior acoustic shadowing, and concomitant changes in the breast nodules are the routine US features that predict malignancy [9,13].

To provide a comprehensive perspective on the ultrasound characteristics of the nodules, specific US manifestations and defined the C-SNs were observed, as follows: The size of the nodule using the maximum transverse diameter (X_6), the longitudinal diameter (X_7) of the largest section perpendicular to each other, and the ratio of longitudinal diameter to transverse diameter (dichotomous variables, >1 or <1) (X_{10}). The lesion shape of the nodules was divided into two categories: Regular and irregular (X_9). The distribution of cyst-solid components was divided into eccentric and regular surrounding (X_{11}). Cystic fluid transmission was categorised as clarity and turbidity (X_{12}). The Cystic-solid intersection was categorised as regular and irregular (X_{13}). The angle between the solid part and the nodule wall was categorised as acute and obtuse (X_{14}). The demarcation of solid-peripheral glands was categorised as clear and unclear (X_{15}). The echo pattern of the solid portion was cat-

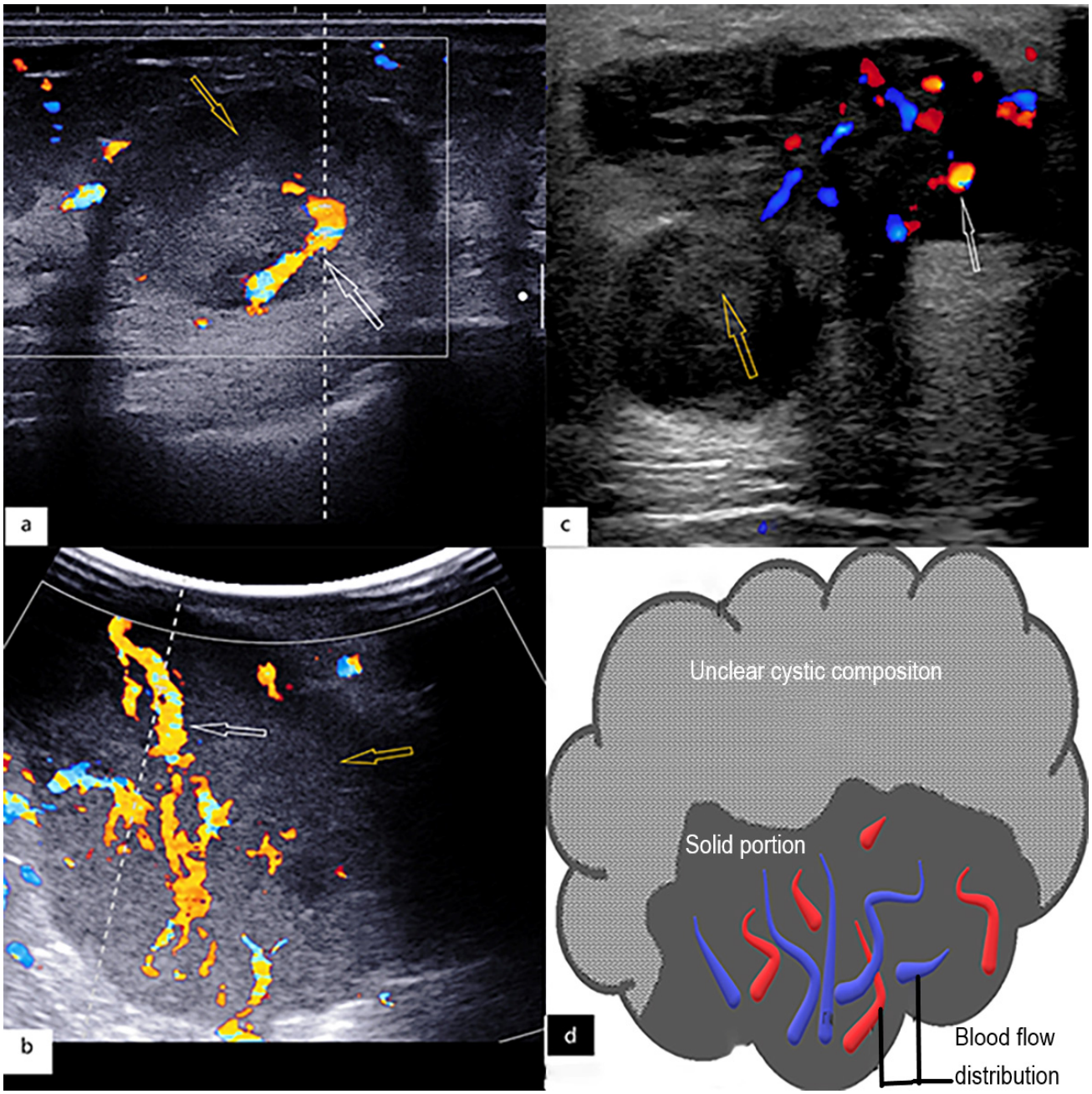

Fig. 5. Patient cases and schematic images present the phenomenon of "Flowers in clouds". Images of (a), (b), and (c) are US feature images, and the image of (d) is a schematic diagram with white arrows representing the BF signal and yellow arrows representing the badly transmissive cystic component.

egorised as hypoechoic and extra hypoechoic (X_{16}). The homogeneity of nodule was categorised as homogeneous and inhomogeneous (X_{17}). The presence of sponge-like structures/capsules was grouped as yes or no (X_{18}). The microcalcification of nodule was categorised as absence and abundant (X_{19}).

The US variables were observed by two physicians with at least 5 years of experience in breast cancer diagnosis [14]. These images without any pathology results were obtained from the hospital picture archiving and communication system (PACS) or ultrasound image workstation of the ultrasonic diagnostic apparatus. The US physicians were blinded to the final pathological diagnosis.

The following clinically relevant variables were combined and assigned. The classification criteria and assignment are shown in Fig. 2 and Table 1.

In this study, the blood flow (BF) was defined and graded using the Adler grading method of general color Doppler. The BF was classified as absent (grade 0), mild (grade 1), moderate (grade 2), or significant (grade 3) according to the region of interest (ROI). No BF was defined as grade 0; Minimal (grade 1) BF was defined as including

Table 1. Assignments and interpretation of clinical and US variables.

Characteristics	Variable	Definition
Nodular malignancy	Y	Yes: Y = 1; No: Y = 0
Clinical Data:		
Age (years)	X_0	Continuous variables
Height (cm)	X_1	Continuous variables
Weight (kg)	X_2	Continuous variables
Lactation history	X_3	Yes: $X_3 = 1$; No: $X_3 = 0$
History of menopause	X_4	Yes: $X_4 = 1$; No: $X_4 = 0$
Family medical history	X_5	Yes: $X_5 = 1$; No: $X_5 = 0$
US characteristics:		
Transverse diameter (mm)	X_6	Continuous variables
Longitudinal diameter (mm)	X_7	Continuous variables
Margin	X_8	Unclear: $X_8 = 1$; Clear: $X_8 = 0$
Lesion shape	X_9	Irregular: $X_9 = 1$; Regular: $X_9 = 0$
Aspect Ratio (Ratio)*	X_{10}	R <1: $X_{10} = 1$; R >1: $X_{10} = 0$
Distribution of cyst-solid components	X_{11}	Eccentric: $X_{11} = 1$; Surrounding: $X_{11} = 0$
Cystic fluid transmission	X_{12}	Poor: $X_{12} = 1$; Clear: $X_{12} = 0$
Cystic-solid intersection	X_{13}	Irregular: $X_{13} = 1$; Regular: $X_{13} = 0$
The angle between solid part and nodule wall	X_{14}	Obtuse angle: $X_{14} = 1$; Acute angle: $X_{14} = 0$
Solid-peripheral glands demarcation**	X_{15}	Unclear: $X_{15} = 1$; Clear: $X_{15} = 0$
Echo pattern of solid portion	X_{16}	Extra Hypoechoic: $X_{16} = 1$; Hypoechoic: $X_{16} = 0$
Homogeneity	X_{17}	Inhomogeneous: $X_{17} = 1$; Homogeneous: $X_{17} = 0$
Presence of sponge-like structures/capsules	X_{18}	Yes: $X_{18} = 1$; No: $X_{18} = 0$
Microcalcification	X_{19}	Yes: $X_{19} = 1$; No: $X_{20} = 0$
Internal vascularity/BF	X_{20}	Abundant: $X_{20} = 1$; Absence: $X_{20} = 0$

*Aspect Ratio is the ratio of the longitudinal diameter to the transverse diameter. **Solid-peripheral gland demarcation is demarcation of the solid portion of the attached cystic wall from the peripheral glands. Homogeneous refers to the cystic part. R, Ratio; BF, Blood flow; US, Ultrasound.

Table 2. Adler grading and assignment.

Levels of blood flow	Definitions
Absence ($X_{20} = 0$):	
Grade 0	No blood flow detected
Grade 1	1 or 2 pixels containing blood flow signals (diameter <0.1 cm)
Abundant ($X_{20} = 1$):	
Grade 2	Multiple small vessels or 1 main vessel
Grade 3	≥4 vessels

one or two pixels containing BF signals (<0.1 cm in diameter); Moderate (grade 2) BF included multiple small vessels or one main vessel; And significant (grade 3) BF included four or more vessels [15]. To simplify the equation flow, make a comparison, and reduce the subjective bias of the operator, grades 0 and 1 were defined as absent BF ($X_{20} = 0$), and grades 2 and 3 were defined as abundant BF ($X_{20} = 1$). The grades are described in Fig. 3 and Table 2.

To reduce bias, two sonographers with >5 years of experience in breast US diagnosis independently assessed the US characteristic variables before surgery or biopsy, and

Table 3. Basic characteristics of the patients and US features of the lesions (Training group).

Characteristics	Training group		t-value/χ^2	p-value
	Benign (n = 74)	Malignant (n = 35)		
Age (years)	42.8 ± 9.9	55.5 ± 13.3	–5.57	<0.01
Height (cm)	160.0 ± 5.2	157.4 ± 6.4	2.08	0.05
Weight (kg)	58.92 ± 7.9	61.1 ± 7.6	–1.38	0.17
Transverse diameter (mm):				
Median [IQR]	11.7 [8.7–15.3]	35.0 [22.3–46.8]	–7.04	<0.01
Longitudinal diameter (mm):				
Median [IQR]	6.7 [4.9–9.6]	20.0 [14.6–32.8]	–6.91	<0.01
Aspect Ratio (Ratio)*:				
Ratio <1	73 (98%)	32 (91%)	3.50	0.09
Ratio ≥1	1 (2%)	3 (9%)		
Lactation history, n (%):				
No	11 (14.9%)	0 (0%)	5.78	0.01
Yes	63 (85.1%)	35 (100%)		
History of menopause, n (%):				
No	56 (76%)	17 (49%)	7.89	<0.01
Yes	18 (24%)	18 (51%)		
Family medical history, n (%):				
No	72 (97%)	34 (97%)	<0.01	1.0
Yes	2 (3%)	1 (3%)		
Margin, n (%):				
Clear	56 (78%)	14 (40%)	13.16	<0.01
Unclear	18 (24%)	21 (60%)		
Lesion shape, n (%):				
Regular	43 (58%)	7 (20%)	13.89	<0.01
Irregular	31 (42%)	28 (80%)		
Distribution of cyst-solid components, n (%):				
Surrounding	31 (42%)	5 (14%)	8.19	<0.01
Eccentric distribution	43 (58%)	30 (86%)		
Cystic fluid transmission, n (%):				
Clarity	66 (84%)	6 (40%)	21.58	<0.01
Bad	8 (16%)	29 (60%)		
Cystic-solid intersection, n (%):				
Regular	30 (41%)	7 (20%)	4.47	0.05
Irregular	44 (60%)	28 (80%)		
Angle between solid part and nodule wall, n (%):				
<90°	42 (57%)	14 (40%)	2.67	0.15
≥90°	32 (43%)	21 (60%)		
Solid-peripheral glands demarcation**, n (%):				
Clear	67 (91%)	28 (80%)	2.36	0.14
Unclear	7 (9%)	7 (20%)		
Echo pattern of solid portion, n (%):				
Hypoechoic	74 (100%)	33 (94%)	4.31	0.10
Extra Hypoechoic	0 (0%)	2 (6%)		
Homogeneity, n (%):				
Homogeneous	33 (44.6%)	10 (28.6%)	2.55	0.14
Inhomogeneous	41 (55.4%)	25 (71.4%)		
Presence of sponge-like structures/capsules, n (%):				
No	58 (78%)	20 (57%)	5.26	0.04
Yes	16 (22%)	15 (43%)		
Microcalcification, n (%):				
No	61 (82 %)	25 (71%)	1.73	0.21
Yes	13 (18%)	10 (29%)		
Internal vascularity/BF, n (%):				
Absent	69 (82%)	8 (49%)	13.39	<0.01
Abundant	5 (18%)	27 (91%)		

*Aspect Ratio is the ratio of the longitudinal diameter to the transverse diameter. **Solid-peripheral gland demarcation is the demarcation of the solid portion of the attached cystic wall from the peripheral glands. Homogeneous refers to the cystic part. BF, Blood flow; IQR, Interquartile range.

Table 4. Basic characteristics of the patients and US features of the lesions (Validation group).

Characteristics	Validation group		t-value/χ^2	p-value
	Benign (n = 44)	Malignant (n = 24)		
Age (years)	43.9 ± 11.7	52.8 ± 12.7	–1.95	0.06
Height (cm)	160.2 ± 4.9	157.8 ± 6.8	1.72	0.09
Weight (kg)	58.8 ± 8.7	60.4 ± 6.8	–0.76	0.45
Transverse diameter (mm):				
Median [IQR]	9.9 [7.6–13.3]	19.8 [11.4–33.3]	–3.71	<0.01
Longitudinal diameter (mm):				
Median [IQR]	5.5 [4.2–6.4]	12.05 [8.8–21.8]	–4.72	<0.01
Aspect Ratio (Ratio)*:				
Ratio <1	44 (100%)	24 (100%)	——	——
Ratio ≥1	——	——		
Lactation history, n (%):				
No	18 (40%)	7 (29%)	0.92	0.43
Yes	26 (60%)	17 (71%)		
History of menopause, n (%):				
No	32 (72%)	13 (54%)	2.39	0.18
Yes	12 (28%)	11 (46%)		
Family medical history, n (%):				
No	37 (84%)	20 (83%)	0.01	1.00
Yes	7 (16%)	4 (17%)		
Margin, n (%):				
Clear	38 (86%)	6 (25%)	25.61	<0.01
Unclear	6 (14%)	18 (75%)		
Lesion shape, n (%):				
Regular	24 (54%)	5 (20%)	7.21	0.01
Irregular	20 (46%)	19 (80%)		
Distribution of cyst-solid components, n (%):				
Surrounding	31 (70%)	6 (25%)	12.94	<0.01
Eccentric distribution	13 (30%)	18 (75%)		
Cystic fluid transmission, n (%):				
Clarity	33 (75%)	6 (25%)	15.87	<0.01
Bad	11 (25%)	18 (75%)		
Cystic-solid intersection, n (%):				
Regular	12 (27%)	10 (41%)	1.47	0.28
Irregular	32 (63%)	14 (59%)		
Angle between solid part and nodule wall, n (%):				
<90°	26 (59%)	14 (58%)	<0.01	1.00
≥90°	18 (41%)	10 (42%)		
Solid-peripheral glands demarcation**, n (%):				
Clear	41 (93%)	21 (88%)	0.62	0.66
Unclear	3 (7%)	3 (12%)		
Echo pattern of solid portion, n (%):				
Hypoechoic	40 (90%)	20 (83%)	0.86	0.44
Extra Hypoechoic	4 (10%)	4 (17%)		
Homogeneity, n (%):				
Homogeneous	18 (41%)	12 (50%)	0.52	0.61
Inhomogeneous	26 (59%)	12 (50%)		
Presence of sponge-like structures/capsules, n (%):				
No	28 (63%)	18 (75%)	0.92	0.42
Yes	16 (37%)	6 (25%)		
Microcalcification, n (%):				
No	38(86%)	18 (75%)	1.38	0.32
Yes	6 (14%)	6 (25%)		
Internal vascularity/BF, n (%):				
Absent	31 (70%)	7 (29%)	10.74	<0.01
Abundant	13 (30%)	17 (71%)		

*Aspect Ratio is the ratio of the longitudinal diameter to the transverse diameter. **Solid-peripheral gland demarcation is the demarcation of the solid portion of the attached cystic wall from the peripheral glands. Homogeneous refers to the cystic part. BF, Blood flow; IQR, Interquartile range.

Table 5. The Statistical results of the traditional model.

Characteristics	β	SE	OR	95% CI	p value
Age	0.11	0.05	1.11	1.01–1.23	0.04*
Longitudinal diameter	0.40	0.09	1.49	1.24–1.81	<0.01*
Cystic fluid transmission	2.24	0.92	9.40	1.56–56.78	0.02*
BF	1.97	0.92	7.16	1.17–43.67	0.03*

β, Regression coefficient; SE, Standard error; OR, Odds ratio; CIs, Confidence intervals; BF, Blood flow distribution. *indicates statistically significant difference.

the subjective variable X_{6-23} was subjected to coherence analysis to calculate the kappa value. Any disagreement on the suitability of a trial for inclusion in the review was resolved by a consensus through discussion.

Statistical Analysis

Statistical analysis was performed using Statistical Package for the Social Sciences (SPSS) version 23.0 (SPSS Inc., Chicago, IL, USA). Normally distributed continuous data were described as mean $\pm$ standard deviation and compared using the independent samples *t*-test. Continuous data that did not fit a normal distribution were described as the median [interquartile range] (IQR) and compared using Mann-Whitney U tests. Categorical data were described as frequency (%) and compared using the chi-squared test, resorting to the Mann-Whitney U test when frequencies <5 were observed in $\geq$20% of cells and Fisher's exact test for comparisons that fitted 2×2 tables. Potential risk factors were evaluated in a two-step analysis, using univariate analysis, to screen variables for consideration, then multivariate analysis to evaluate the screened variables as predictors of reactions.

A total of 109 out of 177 (61.58%) cystic-solid breast nodes comprised the model training group (data from 2018–2020), and logistic forward stepwise analysis selected meaningful variables to establish a risk prediction model (inclusion criteria: $p < 0.05$, exclusion criteria: $p > 0.1$). The Wald chi-squared test was applied to the regression parameter estimates, and Hosmer–Lemeshow goodness-of-fit test was used to assess the overall goodness of fit of the models.

The 68 complex C-SNs (collected in 2021) comprised the model validation group, and the accuracy, sensitivity, specificity, positive and negative predictive value and odds ratio were calculated to validate the model. The receiver operating characteristic (ROC) curve analysis was applied to calculate the area under the curve, so as to evaluate the diagnostic efficacy of each variable entering the model and the whole model, respectively. A p value <0.05 was set to indicate statistically significant difference.

Results

Baseline Characteristics

A total of 177 nodules (including the training and the validation groups) with complex C-SNs of the breast were analyzed. Among these, 118 (67%) were patients with benign nodules, and 59 (32%) were with malignant nodules (Tables 3 and 4). Atypical lesion and borderline phyllodes tumors were classified as benign in this study.

Patients with malignant nodules were older than those with benign nodules (55.5 ± 13.3 *vs.* 42.8 ± 9.9 years, $p < 0.01$). However, no significant difference was observed in height and weight (height: $p > 0.05$; Weight: $p = 0.17$).

The agreement between the two US physicians was analyzed using the Kappa test. The Kappa value was 0.71, indicating a high concordance. Malignant lesions were significantly more frequently seen in nodules with badly transmissive cystic sections (29/44, 60%), compared to the nodules with better transmissivity (6/44, 40%, $p < 0.05$). Also, for nodules with abundant BF signal, malignant nodes were found significantly more frequently than those with less absence of BF signal (27/35, 91% *vs.* 8/35, 9%, $p < 0.05$). With univariate analysis, variables with statistically significant differences ($p < 0.05$) (Table 3) were used as independent variables in the logistic regression.

Multiple Factors Analysis and Model Building

Multivariable logistic regression analysis showed that the BF profile of complex C-SNs (X_{20}; Odds ratio (OR): 7.16; 95% confidence interval (CI): 1.17–43.67; $p = 0.03$), cystic fluid transmission (X_{12}; OR: 9.40; 95% CI: 1.55–56.77; $p = 0.02$), longitudinal diameter (X_7; OR: 1.49; 95% CI: 1.23–1.81; $p < 0.01$), and age (X_0; OR: 1.11; 95% CI: 1.00–1.23; $p = 0.03$) were independent risk factors for malignancy (Table 5). The score M value was calculated according to the logistic regression transformation equation with the following formula: $Z = -12.14 + 2.24 \times X_{12} + 1.97 \times X_{20} + 0.40 \times X_7 + 0.11 \times X_0$; $M = \frac{e^z}{1} + e^z$ (M is the malignancy score, $e = 2.72$).

Model Validation

Hosmer–Lemeshow test was used to evaluate the goodness-of-fit of the regression model, $p = 0.95$, indicating a good fitting effect. The coefficient of determination R^2 was 0.81, indicating high accuracy of the model prediction.

The results of the model calculation for 68 complex C-SNs of the breast were compared to the pathological gold standard, and the ROC curve analysis of the model is shown in Fig. 4. The area under the curve (AUC) of the whole model was 0.89, and the optimal cut-off value of the model was calculated using the Youden index. Thus, it can be concluded that the sensitivity of the model is 88% when the M value is 0.1369, the specificity is 84%, the positive predictive value is 75%, and the negative predictive value is 93%.

Discussion

In the present study, the univariate comparison revealed that the clinical and US characteristics of benign and malignant solid breast nodules were also applicable to the determination of benign and malignant complex cystic nodules [16]. For example, age, breastfeeding history, menopausal history, and characteristics, such as nodule margins, morphology, and BF, are critical features in determining the benignity and malignancy of breast nodules; Also, these features differ significantly in the benign and malignant presentation of C-SNs [7]. The difference is that there are specific signs of C-SNs that cannot be demonstrated in solid nodules, such as cystic partial transmission and the regularity of the cystic-solid interface within the nodule, as these are not clearly described in the BI-RADS classification [5].

The characteristics of BF distribution in breast nodules are vital indicators to determine whether the nodules are benign or malignant [17,18], which is consistent with the results of the current study. The more abundant the BF and the denser the color Doppler BF distribution, the more likely the nodule is malignant [19,20]. Stadlbauer *et al*. [21] used magnetic resonance imaging to evaluate hypoxia and neovascularization and found that malignant nodules are sensitive to oxygen supply, such that during lack of blood supply, there is partial liquefaction and necrosis inside the nodule, forming an atypical cystic nodule. In the complex cystic and solid breast lesions, the risk of malignancy is approximately seven times higher (OR: 7.16; 95% CI: 1.17–43.67; $p = 0.03$) in nodules with abundant BF (Adler classification: Grade 2–3) than in those without abundant BF (Adler classification: Grade 0–1).

This study showed that nodules with a badly transmissive cystic component of the cystic-solid breast nodules and a fine dot floating in the liquid component were about nine times more likely to be malignant nodules (OR: 9.40; 95% CI: 1.55, 56.77; $p = 0.02$) than those with a better transmissive liquid component. Abundant BF in malignant C-SNs of the breast makes them prone to bleeding, leading to clouding of the cystic component, which is reflected in the US image as poor transmission. In a previously published case report by Ko *et al*. [22], a case of spontaneous bleeding from a post-traumatic breast nodule was detected, which recurred after fluid aspiration and was confirmed to be recurrent bleeding due to invasive papillary carcinoma.

The size of the cystic nodules in this study was a major factor that significantly influenced the nature of the nodules, especially the longitudinal diameter of the nodules, which was a risk factor for malignant nodules. In addition, a significantly high frequency of malignant nodules was noted when the longitudinal diameter was >10 mm (34/54, 63%). This phenomenon could be related to a rapid growth rate of malignant nodules. The solid part of the C-SNs grows continually in contradiction to the insufficient blood and oxygen supply, and the solid part liquefies continually, followed by bleeding, necrosis, and a gradual increase in the tension and size of the nodules [23,24]. This finding is consistent with our findings that the larger the longitudinal diameter, the more likely the nodule is to be malignant [25].

Furthermore, the US features of malignant cystic-solid breast nodules were summarized and termed the phenomenon of “flowers in clouds”. The “cloud” refers to the bad transmission of the cystic component of the nodule, while the “flower” refers to the abundant BF signal in the solid part of the nodule. This is a specific US sign that can simplify the process of determining malignant nodules. This sign reflects the “M value” on the ultrasound image. The summary is shown in Fig. 5.

Previous studies concluded that age is an independent risk factor for malignant nodules in the breast [16,26,27]. The results of the present study are consistent with the finding that age is an independent risk factor for malignant nodules. Some studies showed that a history of breastfeeding reduces the likelihood of breast cancer, which is inconsistent with the results obtained in this study, and the phenomenon could be attributed to the and uneven age distribution of participants [28]. The US features, such as microcalcifications, nodule morphology, margins, and other variables that did not enter the equation, were highly suspected of malignant nodules, which might be attributed to phenomena of complex cystic nodules, BF, cystic fluid transmission, longitudinal diameter, and age.

Finally, based on the above independent risk factors, a risk prediction model was developed to predict malignant cystic-solid breast nodules. The prediction models not only improve the probability of correct prediction by evaluating the whole sample and the population but also rapidly predict the risk of malignant nodules in individual subjects. Such risk prediction models have shown discriminatory abilities [29]. In this study, when the M value was >0.14, the probability of having a malignant nodule was increased. The risk scoring model is simple and efficient to implement in clinical studies and can initially assist surgeons in identifying high-risk populations with a relatively objective approach. Hence, it is advocated that patients with an M value >0.14 need to be investigated further to rule out the malignant nodes according to the risk score model.

Nevertheless, the current study has some limitations. First, as a retrospective study, selection bias was mostly unavoidable. Second, the age and weight of the participants in this study were not distributed evenly, which affected the accuracy of the model to a certain extent. Hence, factors such as age and weight should be reduced in the follow-up study.

Conclusions

In conclusion, the findings suggested that the BF in the nodule, the translucency of the cystic portion, and the longitudinal diameter of the nodule are independent risk factors for malignant nodules. This finding awaits prospective multicenter studies to elucidate and establish its value for clinical day to day clinical practice.

Informed Consent

This study is a retrospective study. All the cases collected are the imaging and clinical biochemical data of patients with cystic and solid nodules of the breast revealed by previous ultrasound examinations in the ultrasound department of Zhejiang Provincial People's Hospital. The relevant data included hide the patient's name, age and image number to ensure that the key information of the patient is not disclosed. The results of this study will not be reported to the subjects and will not be used for patient management after being treated as evaluation samples according to the methods specified in the scheme. Therefore, the subjects will not have any risk of false negative and false positive.

Abbreviations

US, Ultrasound; C-SNs, Cystic and solid nodules; ROC, Receiver operating characteristic; BF, Blood flow; AUC, Area under the receiver-operating characteristic curve; BI-RADS, Breast Imaging Reporting and Data system; IQR, Interquartile range.

Availability of Data and Materials

The datasets generated and analyzed during this study are not publicly available due to the requirements from the Ministry of Health of China of the guideline for the ethic review of biomedical research involving human subject (2016), but are available from the corresponding author on reasonable request.

Author Contributions

HL, JLT and CJH—designed the research study; HL and JLT—performed the research; CJH, ANL, KFL, YL and PD—provided help and advice on the data acquisition; HL and JLT—analyzed the data. All authors contributed to editorial changes in the manuscript. All authors read and approved the final manuscript. All authors have participated sufficiently in the work and agreed to be accountable for all aspects of the work.

Ethics Approval and Consent to Participate

All procedures performed in studies involving human participants were in accordance with the ethical standards of the the Ethics Committee of Zhejiang Provincial People's Hospital and with the 1964 Helsinki declaration and its later amendments or comparable ethical standards. Our ethical approval number is 2021QT356. Approved by the Ethics Committee of Zhejiang people's Hospital, informed consent from the patients was waived.

Acknowledgement

Not applicable

Funding

This work was supported by Zhejiang Province Education Department Project (No. Y202146098).

Conflict of Interest

The authors declare no conflict of interest.

References

[1] Siegel RL, Miller KD, Fuchs HE, Jemal A. Cancer statistics, 2022. *CA Cancer J Clin.* 2022;72(1):7–33. doi: 10.3322/caac.21708

[2] Guo R, Lu G, Qin B, Fei B. Ultrasound Imaging Technologies for Breast Cancer Detection and Management: A Review. *Ultrasound Med Biol.* 2018;44(1):37–70. doi: 10.1016/j.ultrasmedbio.2017.09.012

[3] Sood R, Rositch AF, Shakoor D, *et al*. Ultrasound for Breast Cancer Detection Globally: A Systematic Review and Meta-Analysis. *J Glob Oncol.* 2019;5:1–17. doi: 10.1200/JGO.19.00127

[4] Berg WA, Sechtin AG, Marques H, Zhang Z. Cystic breast masses and the ACRIN 6666 experience. *Radiol Clin North Am.* 2010;48(5):931–987. doi: 10.1016/j.rcl.2010.06.007

[5] Spak DA, Plaxco JS, Santiago L, Dryden MJ, Dogan BE. BI-RADS® fifth edition: A summary of changes. *Diagn Interv Imaging.* 2017;98(3):179–190. doi: 10.1016/j.diii.2017.01.001

[6] Choi JS. [Breast Imaging Reporting and Data System (BI-RADS): Advantages and Limitations]. *J Korean Soc Radiol.* 2023;84(1):3–14. doi: 10.3348/jksr.2022.0142

[7] Berg WA, Campassi CI, Ioffe OB. Cystic lesions of the breast: sonographic-pathologic correlation. *Radiology.* 2003;227(1):183–191. doi: 10.1148/radiol.2272020660

[8] Tea MK, Grimm C, Fink-Retter A, *et al*. The validity of complex breast cysts after surgery. *Am J Surg.* 2009;197(2):199–202. doi: 10.1016/j.amjsurg.2007.11.028

[9] Chen M, Zhan WW, Wang WP. Cystic breast lesions by conventional ultrasonography: sonographic subtype-pathologic correlation and BI-RADS Assessment. *Arch Med Sci.* 2014;10(1):76–83. doi: 10.5114/aoms.2014.40734

[10] Tamaki K, Ishida T, Miyashita M, *et al*. Breast ultrasonographic and histopathological characteristics without any mammographic abnormalities. *Jpn J Clin Oncol.* 2012;42(3):168–174. doi: 10.1093/jjco/hyr197

[11] Pistolese CA, Tosti D, Citraro D, *et al*. Probably Benign Breast Nodular Lesions (BI-RADS 3): Correlation between Ultrasound Features and Histologic Findings. *Ultrasound Med Biol.* 2019;45(1):78–84. doi: 10.1016/j.ultrasmedbio.2018.09.004

[12] Ethical guidelines for publication in Clinical Hemorheology and Microcirculation: Update 2016. *Clin Hemorheol Microcirc.* 2016;63(1):1–2. doi: 10.3233/CH-162058

[13] Lee BE, Chung J, Cha ES, Lee JE, Kim JH. Role of shear-

wave elastography (SWE) in complex cystic and solid breast lesions in comparison with conventional ultrasound. *Eur J Radiol.* 2015;84(7):1236–1241. doi: 10.1016/j.ejrad.2015.04.005

[14] Günhan-Bilgen I, Memiş A, Ustün EE, Ozdemir N, Erhan Y. Sclerosing adenosis: mammographic and ultrasonographic findings with clinical and histopathological correlation. *Eur J Radiol.* 2002;44(3):232–238. doi: 10.1016/s0720-048x(02)00020-7

[15] Zhu YC, Zhang Y, Deng SH, Jiang Q. A Prospective Study to Compare Superb Microvascular Imaging with Grayscale Ultrasound and Color Doppler Flow Imaging of Vascular Distribution and Morphology in Thyroid Nodules. *Med Sci Monit.* 2018;24:9223–9231. doi: 10.12659/MSM.911695

[16] Zhang Y, Xu HX, Zhao CK, *et al*. Complex cystic and solid breast lesions: Diagnostic performance of conventional ultrasound, strain imaging and point shear wave speed measurement. *Clin Hemorheol Microcirc.* 2018;69(3):355–370. doi: 10.3233/CH-170252

[17] Niu J, Ma J, Guan X, Zhao X, Li P, Zhang M. Correlation Between Doppler Ultrasound Blood Flow Parameters and Angiogenesis and Proliferation Activity in Breast Cancer. *Med Sci Monit.* 2019;25:7035–7041. doi: 10.12659/MSM.914395

[18] Li M, Li Q, Yin Q, Wang Y, Shang JM, Wang LH. Evaluation of color Doppler ultrasound combined with plasma miR-21 and miR-27a in the diagnosis of breast cancer. *Clin Transl Oncol.* 2021;23(4):709–717. doi: 10.1007/s12094-020-02501-9

[19] Catalano O, Raso MM, D'Aiuto M, Illiano LA, Saturnino PP, Siani A. Additional role of colour Doppler ultrasound imaging in intracystic breast tumours. *Radiol Med.* 2009;114(2):253–266. doi: 10.1007/s11547-008-0346-6

[20] Wu C, Pineda F, Hormuth DA 2nd, Karczmar GS, Yankeelov TE. Quantitative analysis of vascular properties derived from ultrafast DCE-MRI to discriminate malignant and benign breast tumors. *Magn Reson Med.* 2019;81(3):2147–2160. doi: 10.1002/mrm.27529

[21] Stadlbauer A, Zimmermann M, Bennani-Baiti B, *et al*. Development of a Non-invasive Assessment of Hypoxia and Neovascularization with Magnetic Resonance Imaging in Benign and Malignant Breast Tumors: Initial Results. *Mol Imaging Biol.* 2019;21(4):758–770. doi: 10.1007/s11307-018-1298-4

[22] Ko KH, Kim EK, Park BW. Invasive papillary carcinoma of the breast presenting as post-traumatic recurrent hemorrhagic cysts. *Yonsei Med J.* 2006;47(4):575–577. doi: 10.3349/ymj.2006.47.4.575

[23] Shen Q, Reedijk M. Notch Signaling and the Breast Cancer Microenvironment. *Adv Exp Med Biol.* 2021;1287:183–200. doi: 10.1007/978-3-030-55031-8_12

[24] Cericatto R, Pozzobon A, Morsch DM, Menke CH, Brum IS, Spritzer PM. Estrogen receptor-alpha, bcl-2 and c-myc gene expression in fibroadenomas and adjacent normal breast: association with nodule size, hormonal and reproductive features. *Steroids.* 2005;70(3):153–160. doi: 10.1016/j.steroids.2004.10.013

[25] Gu Y, Tian JW, Ran HT, *et al*. The Utility of the Fifth Edition of the BI-RADS Ultrasound Lexicon in Category 4 Breast Lesions: A Prospective Multicenter Study in China. *Acad Radiol.* 2022;29 Suppl 1:S26–S34. doi: 10.1016/j.acra.2020.06.027

[26] Biganzoli L, Battisti NML, Wildiers H, *et al*. Updated recommendations regarding the management of older patients with breast cancer: a joint paper from the European Society of Breast Cancer Specialists (EUSOMA) and the International Society of Geriatric Oncology (SIOG). *Lancet Oncol.* 2021;22(7):e327–e340. doi: 10.1016/S1470-2045(20)30741-5

[27] Luan HH, Luo LS, Lu ZY. Historical Trends in Incidence of Breast Cancer in Shanghai, Hong Kong and Los Angeles, 1973–2012: A Joinpoint and Age-Period-Cohort Analysis. *Int J Public Health.* 2021;66:603810. doi: 10.3389/ijph.2021.603810

[28] Qiu R, Zhong Y, Hu M, Wu B. Breastfeeding and Reduced Risk of Breast Cancer: A Systematic Review and Meta-Analysis. *Comput Math Methods Med.* 2022;2022:8500910. doi: 10.1155/2022/8500910

[29] Bargon CA, Young-Afat DA, Ikinci M, *et al*. Breast cancer recurrence after immediate and delayed postmastectomy breast reconstruction-A systematic review and meta-analysis. *Cancer.* 2022;128(19):3449–3469. doi: 10.1002/cncr.34393